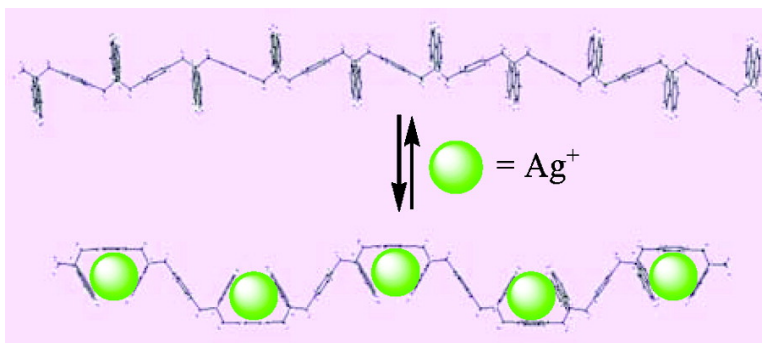


## Convergent Synthesis of Alternating Fluorene-*p*-xylene Oligomers and Delineation of the (Silver) Cation-Induced Folding

Vincent J. Chebny, and Rajendra Rathore

*J. Am. Chem. Soc.*, **2007**, 129 (27), 8458-8465 • DOI: 10.1021/ja0687522 • Publication Date (Web): 16 June 2007

Downloaded from <http://pubs.acs.org> on February 16, 2009



### More About This Article

Additional resources and features associated with this article are available within the HTML version:

- Supporting Information
- Links to the 2 articles that cite this article, as of the time of this article download
- Access to high resolution figures
- Links to articles and content related to this article
- Copyright permission to reproduce figures and/or text from this article

[View the Full Text HTML](#)

## Convergent Synthesis of Alternating Fluorene-*p*-xylene Oligomers and Delineation of the (Silver) Cation-Induced Folding

Vincent J. Chebny and Rajendra Rathore\*

Contribution from the Department of Chemistry, Marquette University, P.O. Box 1881, Milwaukee, Wisconsin 53201-1881

Received December 6, 2006; E-mail: rajendra.rathore@marquette.edu

**Abstract:** Convergent synthetic routes for the preparation of hitherto unknown fluorene-*p*-xylene oligomers (containing up to 10 fluorene moieties) from readily available starting materials are described. The conformationally adaptable monomeric receptor (which is made of a pair of fluorene and one *p*-xylene ring, i.e., **Z1**) undergoes a simple C–C bond rotation in the presence of silver cations to produce a  $\pi$ -prism-like receptor which binds a single silver cation with remarkable efficiency (i.e.,  $K \approx 15\,000\text{ M}^{-1}$ ). The data on  $^1\text{H}$  NMR spectroscopic titrations with  $\text{Ag}^+$  together with the density functional theory and AM1 calculations allows us to establish that various oligomers of **Z1** (i.e., **Z2–Z9**) also undergo ready folding into the structures that contain multiple  $\pi$ -prism-like receptor sites in the presence of silver cations. The multiple cavities in **Z3–Z9** accommodate a single silver cation per cavity with efficiency similar to that of **Z1**.

### Introduction

There are numerous examples in nature where weak inter- and intramolecular bonding interactions (such as hydrogen bonding,<sup>1</sup>  $\pi$ -stacking,<sup>2</sup> Columbic interactions,<sup>3</sup> metal-ion binding,<sup>4</sup> etc.) permit structure modulation of the biopolymers (such as polypeptides, ribonucleic acid, polysaccharides) into well-defined ‘molecular machines’ that perform complex functions from enzymatic catalysis to information storage and retrieval.<sup>5</sup> Furthermore, the design and syntheses of artificial polymeric (organic) materials whose structures can be modulated by external stimuli (such as heat,<sup>6</sup> light,<sup>7</sup> or metal-ion binding<sup>8</sup>) constitute an important area of research owing to the fact that such materials may hold potential for applications in the ever

evolving areas of molecular electronics and nanotechnology.<sup>9</sup> A number of such synthetic materials, generally termed ‘foldamers’, have been prepared and are discussed in detail in a recently published review article by Moore and co-workers.<sup>10</sup>

We recently synthesized<sup>11</sup> a hydrocarbon ligand 1,4-bis(9-methyl-9*H*-fluoren-9-yl)methyl]benzene (**1**, see structure below) from readily available fluorene and  $\alpha,\alpha$ -dichloro-*p*-xylene that possesses a unique molecular structure where a simple C–C single bond rotation converts it from an extended (“**Z**”) conformer to an isoenergetic (folded) delta (“ $\Delta$ ”) conformer, as established by density functional theory (DFT) calculations<sup>11</sup> at the B3LYP/6-31G\* level. The cavity formed by three aromatic walls (i.e., two fluoranyl rings and one *p*-xylyl ring) in the “ $\Delta$ ” conformation of **1** is remarkably similar to that found in  $\pi$ -prism (**2**)<sup>12</sup>—a well-known and efficient receptor for the binding of a variety of metal cations<sup>12,13</sup>—as shown in Figure 1. Although, the energy difference between the two conformers of **1** is only  $\sim 0.4$  kcal/mol, X-ray crystal structure analysis showed that **1** in the solid state exists exclusively as the extended

- (1) (a) Murray, T. J.; Zimmerman, S. C. *J. Am. Chem. Soc.* **1992**, *114*, 4010–4011. (b) Corbin, P. S.; Zimmerman, S. C. *J. Am. Chem. Soc.* **2000**, *122*, 3799. (c) Margulis, C. J.; Stern, H. A.; Berne, B. J. *J. Phys. Chem. B* **2002**, *106*, 10748.
- (2) (a) Han, J. J.; Wang, W.; Li, A. J. *J. Am. Chem. Soc.* **2006**, *128*, 672 and references therein. (b) Zych, A. J.; Iverson, B. L. *J. Am. Chem. Soc.* **2000**, *122*, 8898. (c) Nguyen, J. Q.; Iverson, B. L. *J. Am. Chem. Soc.* **1999**, *121*, 2639.
- (3) (a) Gabriel, G. J.; Sorey, S.; Iverson, B. L. *J. Am. Chem. Soc.* **2005**, *127*, 2637. (b) Shepherd, N. E.; Abbenante, G.; Fairlie, D. P. *Angew. Chem., Int. Ed.* **2004**, *43*, 2687. (c) Gellman, S. H. *Acc. Chem. Res.* **1998**, *31*, 173.
- (4) (a) Ghadiri, M. R.; Choi, C. *J. Am. Chem. Soc.* **1990**, *112*, 1630. (b) Kelso, M. J.; Hoang, H. N.; Appleton, T. G.; Fairlie, D. P. *J. Am. Chem. Soc.* **2000**, *122*, 10488. (c) Nicoll, A. J.; Miller, D. J.; Futter, K.; Ravelli, R.; Allemann, R. K. *J. Am. Chem. Soc.* **2006**, *128*, 9187.
- (5) (a) Ritz, T.; Park, S.; Schulten, K. *J. Phys. Chem. B* **2001**, *105*, 8259. (b) Stubbe, J.; van der Donk, W. A. *Chem. Rev.* **1998**, *98*, 705 and references therein. (c) Rasmussen, P. H.; Ramanujam, P. S.; Hvilsted, S.; Berg, R. H. *J. Am. Chem. Soc.* **1999**, *121*, 4738. (d) Alonso, M.; Reboto, V.; Guiscardo, L.; San, Martin, A.; Rodriguez-Cabello, J. C. *Macromolecules* **2000**, *33*, 9480.
- (6) Margulis, C. J.; Stern, H. A.; Berne, B. J. *J. Phys. Chem. B* **2002**, *106*, 10748 and references therein.
- (7) (a) Balbo, Block, M. A.; Hecht, S. *Macromolecules* **2004**, *37*, 4761. (b) Khan, A.; Kaiser, C.; Hecht, S. *Angew. Chem., Int. Ed.* **2006**, *45*, 1878. (c) McQuade, T. D.; Pullen, A. E.; Swager, T. M. *Chem. Rev.* **2000**, *100*, 2537.

- (8) (a) Chang, K.-J.; Kang, B.-N.; Lee, M.-H.; Jeong, K.-S. *J. Am. Chem. Soc.* **2005**, *127*, 12215. (b) Suzuki, Y.; Morozumi, T.; Nakamura, H.; Shimomura, M.; Hayashita, T.; Bartsh, R. A. *J. Phys. Chem. B* **1998**, *102*, 7910. (c) Ghosh, S.; Ramakrishnan, S. *Macromolecules* **2005**, *38*, 676. (d) Piguet, C.; Bernardinelli, G.; Hopfgartner, G. *Chem. Rev.* **1997**, *97*, 2005 and references therein. (e) Zhang, F.; Bai, S.; Yap, G. P. A.; Tarwade, V.; Fox, J. M. *J. Am. Chem. Soc.* **2005**, *127*, 10590.
- (9) *Introduction to Molecular Electronics*; Petty, M. C.; Bryce, M. R., Bloor, D., Eds.; Oxford University Press: New York, 1995.
- (10) Hill, D. J.; Mio, M. J.; Prince, R. B.; Hughes, T. S.; Moore, J. S. *Chem. Rev.* **2001**, *101*, 3893 and references within. Also see: Schmuck, C. *Angew. Chem., Int. Ed.* **2003**, *42*, 2448. Huc, I. *Eur. J. Org. Chem.* **2004**, 17.
- (11) Rathore, R.; Chebny, V. J.; Abdelwahed, S. A. *J. Am. Chem. Soc.* **2005**, *127*, 8012.
- (12) (a) Pierre, J. L.; Baret, P.; Chautemps, P.; Armand, M. *J. Am. Chem. Soc.* **1981**, *103*, 2986. (b) Pierre, G.; Baret, P.; Chautemps, P.; Pierre, J. L. *Electrochim. Acta* **1983**, *28*, 1269.

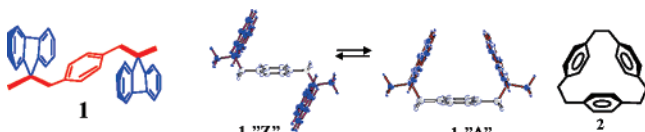


**Figure 1.** Optimized structures of the isoenergetic conformers of **1** by density functional theory (DFT) calculations at B3LYP/6-31G\* level and structural similarity with tris[2.2.2]-paracyclophane or  $\pi$ -prismand (**2**).

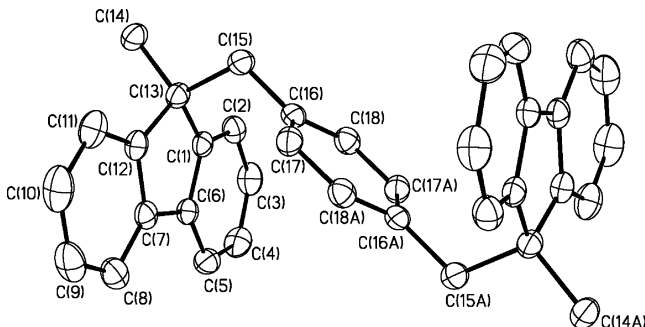
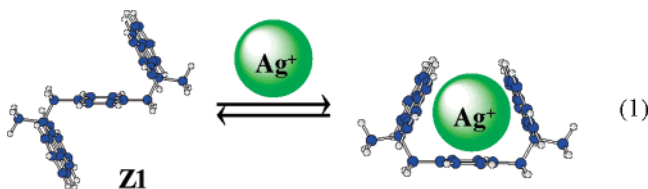


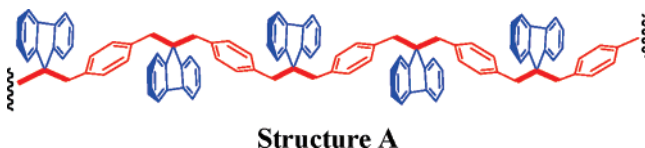
**Figure 2.** X-ray structure of **1** showing the extended conformer.

“Z” conformer (Figure 2). Note that the X-ray structure of **1** was completely in accord with the calculated structure shown in Figure 1.

Moreover, variable-temperature  $^1\text{H}$  NMR analyses of **1** indicated that its two conformers (i.e., extended, **Z**, and folded,  $\Delta$ ) cannot be frozen out at lower temperatures (i.e., ca.  $-90$   $^\circ\text{C}$ ). However, the conformational adaptability of **1**, which hereafter will be referred to as **Z1**, allows it to bind a single silver cation into the cavity of the  $\Delta$  conformer with an excellent efficiency ( $K \approx 15\,000\ \text{M}^{-1}$ ), i.e., eq 1.<sup>11</sup>



It is envisioned that the fluorene-*p*-xylene-based receptor **Z1** (shown above in eq 1) can be easily woven into a hitherto unknown polymeric structure by linking *p*-xylene groups at carbon 9 of the fluorene moieties, i.e., structure **A**.



Accordingly, herein we will report the first preparation of oligomers of structure **A** containing up to 10 fluorene moieties by a convergent synthetic approach. Furthermore, using  $^1\text{H}$

NMR spectroscopy it will be shown that these conformationally adaptable oligomers readily fold into the structures that contain multiple  $\pi$ -prismand-like receptor sites (which are made of a pair of fluorene and one *p*-xylene ring) in the presence of silver cations as follows.

## Results and Discussion

**Synthesis of Fluorene-*p*-xylene Oligomers.** The initial attempt (**P1**) to polymerize fluorene with  $\alpha,\alpha$ -dichloro-*p*-xylene in the presence of potassium *tert*-butoxide as a base in tetrahydrofuran at  $0$   $^\circ\text{C}$  led to a cream-colored solid which melted at  $270$ – $274$   $^\circ\text{C}$ , and its structure was inferred by  $^1\text{H}/^{13}\text{C}$  NMR spectroscopy to be a mixture of cyclic oligomers (structure **B**), i.e. Scheme 1, reaction **P1**.

A similar mixture of cyclic oligomers (structure **B**) was obtained upon reactions of various mixtures of fluoranyl and  $\alpha,\alpha$ -dichloro-*p*-xylyl derivatives (vide infra) in Scheme 1 (i.e., reactions **P2**–**P5**) in tetrahydrofuran in the presence of potassium *tert*-butoxide as a base, as confirmed by the observation of fairly narrow signals in the rather simple  $^1\text{H}/^{13}\text{C}$  NMR spectra, in each case, as shown in Figure 3.<sup>14</sup>

The identity of the similar mixtures of cyclic oligomers, obtained in various reactions in Scheme 1, was further confirmed by MALDI-TOF mass spectrometry (see Figure S1 in the Supporting Information).

Thus, an unexpected formation of cyclic oligomers in Scheme 1 necessitated development of a different synthetic approach for preparation of acyclic oligomers (structure **A**) as follows.

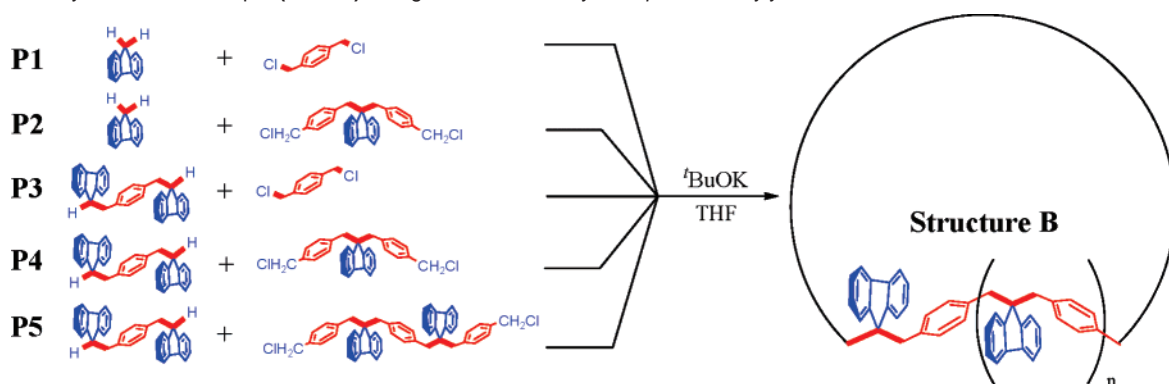
The syntheses of acyclic oligomers containing up to 10 fluorene units were accomplished by a stepwise (convergent) synthetic approach. The key to the success of this (controlled) approach lies in the fact that carbon 9 of fluorene can be selectively mono- or dialkylated by a simple variation of the reaction conditions and thus allowed straightforward access to the fragments required for designing convergent routes to the various acyclic oligomers **Z1**–**Z9** (Scheme 2).

Thus, a highly selective monolithiation of fluorene in anhydrous tetrahydrofuran using *n*-BuLi at  $-78$   $^\circ\text{C}$  followed by reaction with an alkyl halide [such as iodomethane, ethyl-4-(bromomethyl)benzoate, or  $\alpha,\alpha$ -dichloro-*p*-xylene] led to quantitative formation of the initial building blocks as shown in Scheme 2 (bottom). [Note that the combination of notations **F**, **H**, **M**, **E**, **A**, **C**, and **X** with numeral subscripts for various intermediates in Scheme 2 refers to the number of fluorenes, hydrogens, methyls, ester, alcohol, chloro, and xylyl groups, respectively.]

The second lithiation of the initial building blocks in Scheme 2, in the same pot or after isolation of the products, using *n*-BuLi at  $-78$   $^\circ\text{C}$  in THF followed by reaction with ethyl-4-(bromomethyl)benzoate afforded the ester building blocks that were easily converted into their corresponding benzyl chlorides by a simple two-step procedure. For example, reduction of the esters using lithium aluminum hydride in refluxing THF followed by reaction of the resulting alcohol with thionyl chloride in chloroform at  $\sim 0$   $^\circ\text{C}$  afforded the corresponding benzyl chlorides in almost quantitative yields. Various benzyl chlorides

(13) Kang, H. C.; Hanson, A. W.; Eaton, B.; Boelheide, V. *J. Am. Chem. Soc.* **1985**, *107*, 1979. Also see: (a) Heirtzler, F. R.; Hopf, H.; Jones, P. G.; Bubenitachek, P.; Lehne, V. *J. Org. Chem.* **1993**, *58*, 2781–2784. (b) Gano, J. E.; Subramaniam, G.; Birnbaum, R. *J. Org. Chem.* **1990**, *55*, 4760. (c) Lindeman, S. V.; Rathore, R.; Kochi, J. K. *Inorg. Chem.* **2000**, *39*, 5707. (d) Prodi, L.; Bolletta, F.; Montalti, M.; Zaccheroni, N. *Coord. Chem. Rev.* **2000**, *205*, 59–83. (e) Ikeda, M.; Tanida, T.; Takeuchi, M.; Shinkai, S. *Org. Lett.* **2000**, *2*, 1803. (f) Munakata, M.; Wu, L. P.; Kuroda-Sowa, T.; Maekawa, M.; Suenaga, Y.; Sugimoto, K. *Inorg. Chem.* **1997**, *36*, 4903. (g) Munakata, M.; Wu, L. P.; Ning, G. L.; Kuroda-Sowa, T.; Maekawa, M.; Suenaga, Y.; Macao, N. *J. Am. Chem. Soc.* **1999**, *121*, 4968. (h) Yang, R.-H.; Chan, W.-H.; Lee, A. W. M.; Xia, P.-F.; Zhang, H.-K.; Li, K. *J. Am. Chem. Soc.* **2003**, *125*, 2884.

(14) The mixture of cyclic oligomers in Scheme 1 can also bind silver cation with efficiency similar to those observed with various **Zn**'s. We are actively pursuing the isolation of a pure oligomer to delineate its structure and usage for designing functional materials. These results will be described in a future publication.

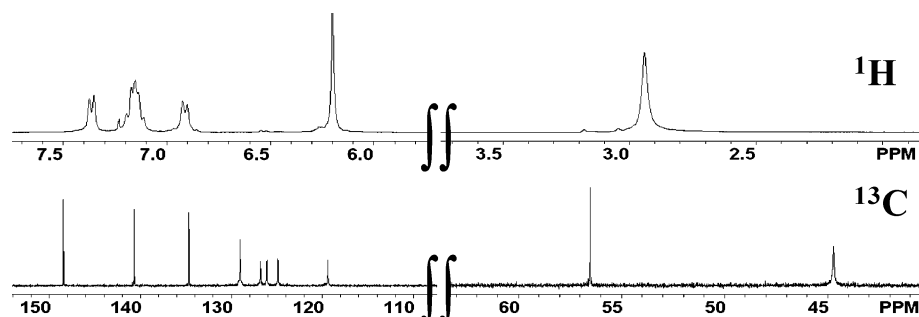
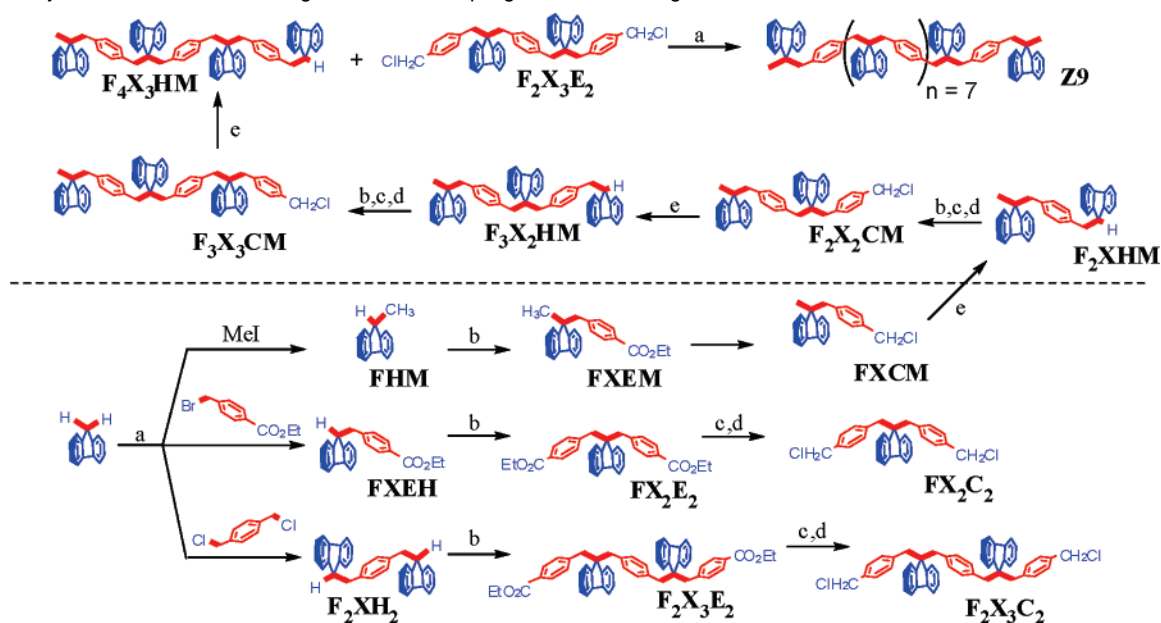
**Scheme 1.** Polymerization Attempts (P1–P5) Using Various Fluoranyl and *p*-Dichloroxylyl Derivatives

in Scheme 2 (bottom) served as internal and capping units for the preparation of various oligomers.

The capping unit **FXCM** can be further elongated by repeating the high-yielding reaction sequence depicted in the Scheme 2 (bottom). Thus, in a one-pot procedure reaction of **FXCM** with the fluoranyl anion (generated from fluorene and *n*-BuLi in THF at  $-78\text{ }^{\circ}\text{C}$ ) followed by addition of another equivalent of *n*-BuLi and ethyl-4-(bromomethyl)benzoate afforded **F<sub>2</sub>X<sub>2</sub>EM** in excellent yield. Reduction of the resulting ester with  $\text{LiAlH}_4$  followed by reaction with thionyl chloride

afforded a higher homologue of the capping unit (i.e., **F<sub>2</sub>X<sub>2</sub>CM**). A similar reaction sequence allowed the preparation of capping units containing three and four fluorene moieties with either an electrophilic benzyl chloride group or a precursor to a nucleophilic fluoranyl anion, i.e., Scheme 2 (top).

The syntheses of linear oligomers **Z2–Z9** were finally accomplished by piecing together various inner building blocks (i.e., fluorene, **F<sub>2</sub>XH<sub>2</sub>**, **FX<sub>2</sub>C<sub>2</sub>**, and **F<sub>2</sub>X<sub>3</sub>C<sub>2</sub>**) and capping units (**FXCM**, **F<sub>2</sub>XHM**, **F<sub>3</sub>X<sub>2</sub>HM**, and **F<sub>4</sub>X<sub>3</sub>HM**) in tetrahydrofuran using

**Figure 3.**  $^1\text{H}/^{13}\text{C}$  NMR spectra of the mixture of cyclic oligomers obtained from Scheme 1 in  $\text{CDCl}_3$  at  $22\text{ }^{\circ}\text{C}$ .**Scheme 2.** Synthesis of Various Building Blocks and Coupling To Form Zn Oligomers<sup>a</sup>

<sup>a</sup> (a) *n*-BuLi/THF/ $-78\text{ }^{\circ}\text{C}$ . (b) *n*-BuLi/ $-78\text{ }^{\circ}\text{C}$ /ethyl-4-(bromomethyl)benzoate. (c)  $\text{LiAlH}_4$ /THF/reflux. (d)  $\text{SOCl}_2/\text{CHCl}_3/0\text{ }^{\circ}\text{C}$ . (e) Fluorene/*n*-BuLi/THF/ $-78\text{ }^{\circ}\text{C}$ .

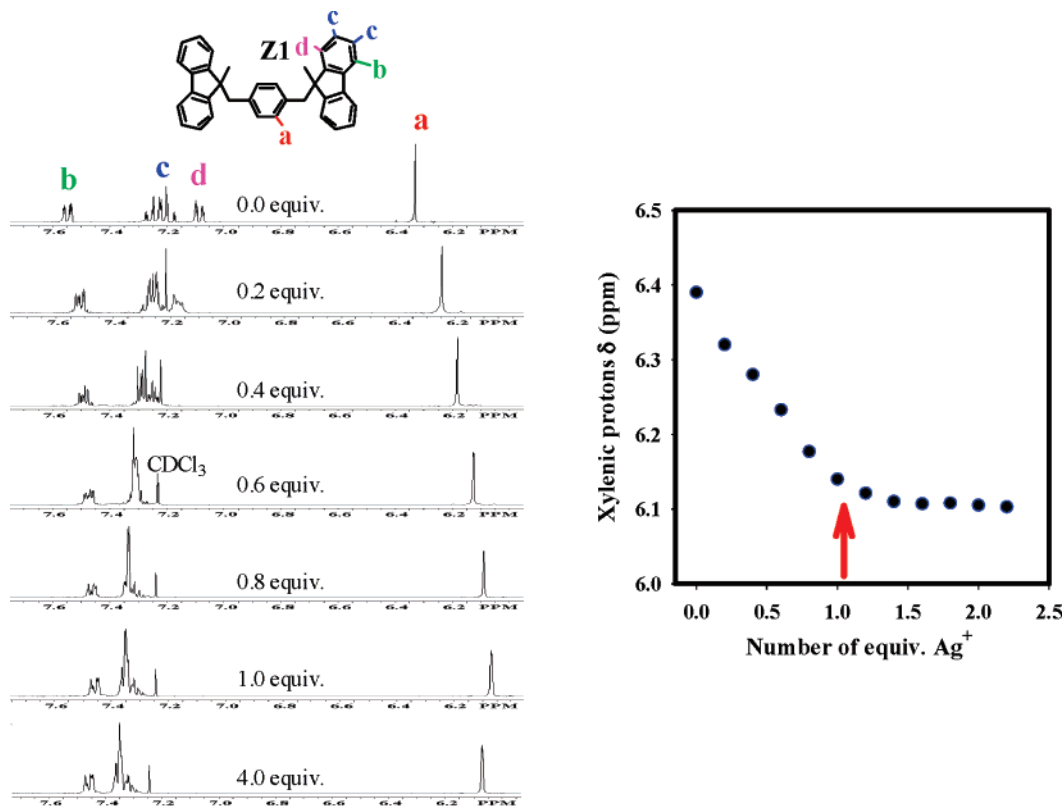


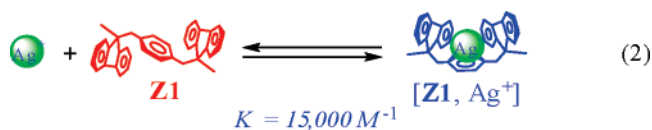
**Figure 4.** (Left) Partial <sup>1</sup>H NMR spectra of **Z1** obtained upon an incremental addition of CF<sub>3</sub>SO<sub>3</sub>Ag in CDCl<sub>3</sub>-CD<sub>3</sub>OD at 22 °C. (Right) Plot of changes in the chemical shifts of the xylene protons (indicated by letter “a” in the structure in the Figure 4A) against the added equivalents of a solution of CF<sub>3</sub>SO<sub>3</sub>Ag in CDCl<sub>3</sub>-CD<sub>3</sub>OD at 22 °C.

potassium *tert*-butoxide as a base at 0 °C in excellent yields as exemplified by the preparation of **Z9** in Scheme 2 (top).

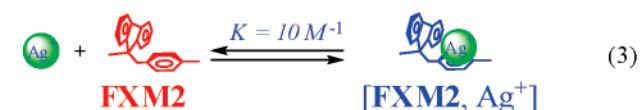
The acyclic oligomers **Z2**–**Z9** were readily purified by filtration through a short pad of silica gel using mixtures of ethyl acetate–hexanes as an eluent and characterized by <sup>1</sup>H and <sup>13</sup>C NMR spectroscopy as well as by mass spectrometry. The <sup>1</sup>H NMR spectra of **Z1**–**Z9** compiled in Figure S2 in the Supporting Information confirmed that an expected ratio of the integrations of the signals due to the methyl protons with that of the methylenic or xylene protons was observed in each case. Moreover, the <sup>1</sup>H NMR spectra of oligomers **Z2**, **Z3**, and **Z4**, with an increasing number of repeating units, showed the expected number of signals for various methylene and xylene protons. Expectedly, further increase of the repeating units in **Z5**–**Z9** showed that the <sup>1</sup>H NMR signals due to the additional methylenic and xylene protons were overlapping with one of the methylenic (2.95 ppm) and xylene (6.20 ppm) signals in the spectrum of **Z4**. The <sup>13</sup>C NMR spectra of various acyclic oligomers **Z1**–**Z9** are also compared in Figure S3 in the Supporting Information.

**Binding of Silver Cation (Ag<sup>+</sup>) to Fluorene-*p*-xylene Oligomers **Z1**–**Z9**.** The binding of silver cation to various acyclic oligomers **Z1**–**Z9** was monitored by <sup>1</sup>H NMR spectroscopy. Thus, the changes in the <sup>1</sup>H NMR spectra of **Z1** in chloroform-*d* (0.05 mM) by an incremental addition of a concentrated solution of silver trifluoromethane–sulfonate (0.5 mM) in 1:1 chloroform-*d*/methanol-*d*<sub>4</sub> showed considerable shifts of the aromatic signals up to addition of 1 equiv of Ag<sup>+</sup>, as shown in Figure 4A. Moreover, the <sup>1</sup>H NMR spectrum remained unchanged upon further addition of Ag<sup>+</sup> solution, i.e., beyond 1 equiv, as shown in Figure 4B.

Efficient binding of a single silver cation by the conformationally adaptable receptor **Z1** was confirmed by a competition experiment with deltapane **2**—a well-known and efficient receptor for silver cation—as well as by a spectrophotometric determination of the binding constant  $K \approx 15\,000\text{ M}^{-1}$  using the Benesi–Hildebrand procedure (see Figure 5A/B).<sup>15</sup> Moreover, the 1:1 complexation stoichiometry for [**Z1**, Ag<sup>+</sup>] was established by Job’s plot analysis (Figure 5C),<sup>16</sup> i.e. eq 2.



It is also important to note that a model compound **FXM2**, containing only one fluoranyl moiety, bound Ag<sup>+</sup> with much less efficiency and required a large excess of Ag<sup>+</sup> for complete utilization of the ligand, and a binding constant  $K \approx 10$  was estimated using <sup>1</sup>H NMR spectroscopy, i.e., eq 3.



Thus, the experiments discussed above demonstrated that **Z1** binds a single silver cation with remarkable efficiency due to the fact that it readily adapts a  $\pi$ -prism-and-like conformation by a simple C–C bond rotation (see also eq 1).

(15) Benesi, H. A.; Hildebrand, J. J. *J. Am. Chem. Soc.* **1949**, *71*, 2703–2707.

(16) Connors, K. A. *Binding Constants*; Wiley: New York, 1987.

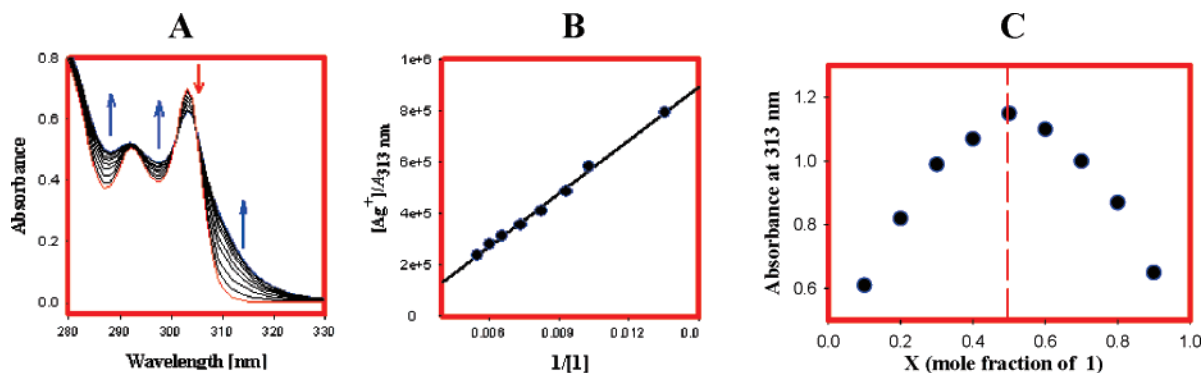


**Figure 5.** (A) Spectra obtained upon incremental addition of a 15 mM solution of  $Ag^+ CF_3SO_3^-$  in methanol (black) to a 0.8 mM solution of **Z1** (red) in  $CH_2Cl_2$  at 22 °C. (B) Benesi–Hildebrand plot of **Z1** and  $Ag^+CF_3SO_3^-$ . (C) Job's plot of a 1:1 complex of **Z1** and  $Ag^+$  cation, where the absorbance at 313 nm was plotted against the mole fraction of **Z1** at an invariant total concentration of 0.02 M in a 19:1 mixture of  $CH_2Cl_2/CH_3OH$  (v/v).

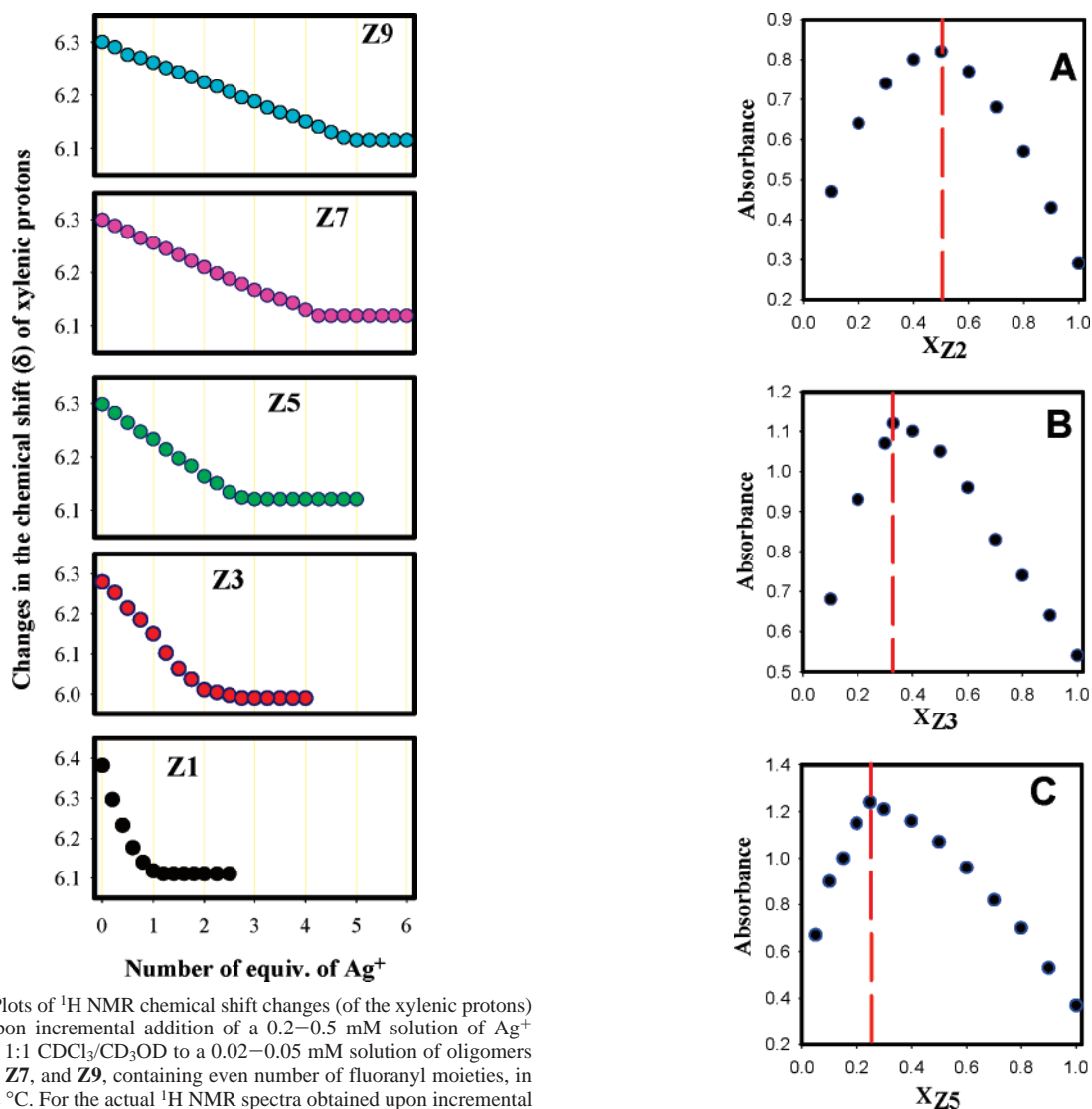


**Figure 6.** Plots of  $^1H$  NMR chemical shift changes (of the xylenic protons) attendant upon incremental addition of a 0.2–0.5 mM solution of  $Ag^+ CF_3SO_3^-$  in 1:1  $CDCl_3/CD_3OD$  to a 0.02–0.05 mM solution of oligomers **Z1**, **Z3**, **Z5**, **Z7**, and **Z9**, containing even number of fluoranyl moieties, in  $CDCl_3$  at 22 °C. For the actual  $^1H$  NMR spectra obtained upon incremental addition of  $Ag^+$  solution, see Figures S8, S10, S12, and S14 in the Supporting Information.

In order to determine the efficiency and binding of silver cations to the higher homologues of **Z1**, similar  $^1H$  NMR spectral titrations of the chloroform- $d$  solutions of **Z3**, **Z5**, **Z7**, and **Z9**, containing an even number of fluorenes (i.e., 4, 6, 8, and 10 fluoranyl moieties, respectively), with a concentrated solution of  $Ag^+ CF_3SO_3^-$  in a 1:1 mixture of chloroform- $d$  and methanol- $d_4$  were carried out at 22 °C; see Figures S8, S10, S12, and

**Figure 7.** Job's plots of a 1:1 complex of **Z2** and  $Ag^+$  cation (A), a 1:2 complex of **Z3** and  $Ag^+$  cation (B), and a 1:3 complex of **Z5** and  $Ag^+$  cation (C). The Job's plots were obtained by plotting the growth of absorbance at 313 nm against the mole fraction of **Z2**, **Z3**, and **Z5**, respectively, at an invariant total concentration of 0.02 M in a 19:1 mixture of  $CH_2Cl_2/CH_3OH$  (v/v).

S14 in the Supporting Information. The reproducible spectral titrations thus obtained showed that **Z3**, **Z5**, **Z7**, and **Z9** bind 2, 3, 4, and 5 equiv of  $Ag^+$ , respectively, as shown in Figure 6.

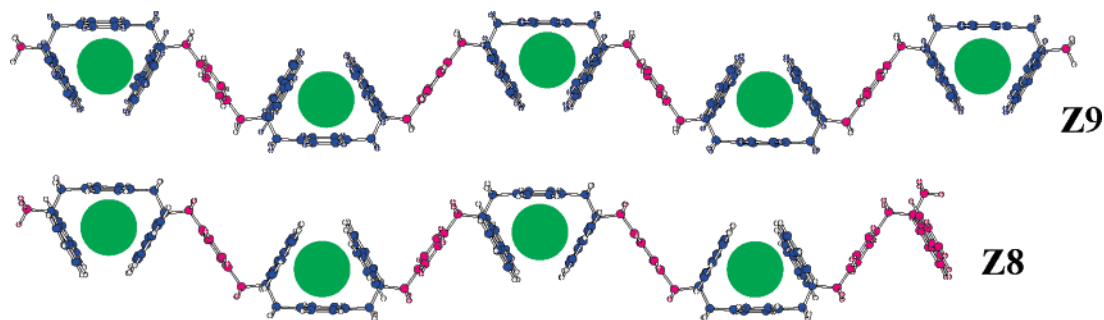


**Figure 8.** Calculated molecular structures of representative examples, i.e., **Z8** and **Z9**, using Spartan (AM1) show formation of multiple  $\pi$ -prismand-like cavities for binding of  $\text{Ag}^+$  cations.

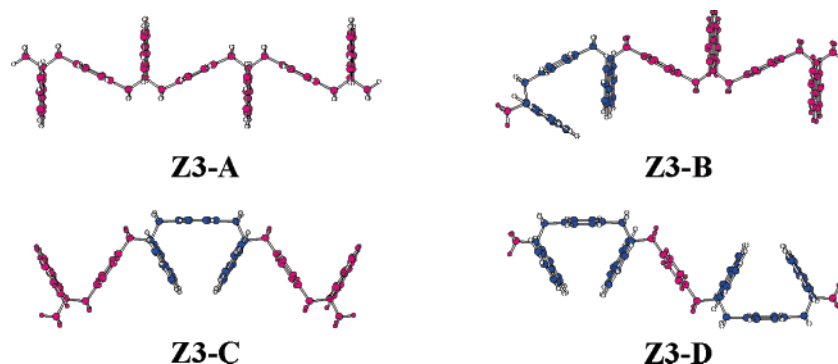


**Figure 9.** Calculated molecular structures of various (almost) isoenergetic conformers of **Z3** using density functional theory calculations at the B3LYP/6-31G\* level.

The  $^1\text{H}$  NMR spectral titrations of homologues **Z2**, **Z4**, **Z6**, and **Z8**, containing an odd number of fluorenes (i.e., 3, 5, 7, and 9 fluoranyl moieties, respectively) with  $\text{Ag}^+ \text{CF}_3\text{SO}_3^-$  showed that these oligomers bind 1, 2, 3, and 4 equiv of silver cations, respectively, as shown in Figure S4 in the Supporting Information.

Additionally, the binding of multiple silver cations to representative **Z<sub>n</sub>** receptors was also probed by Job's plot analyses<sup>16</sup> (see Figure 7). For example, **Z1** (see Figure 5), **Z3**, and **Z5** showed that the maximum of the binding interactions takes place at the mole fraction of 0.5 for **Z1**, 0.33 for **Z3**, and 0.25 for **Z5**, which is consistent with the uptake of 1, 2, and 3  $\text{Ag}^+$  cations by **Z1**, **Z3**, and **Z5**, respectively, by NMR spectroscopy titrations in Figure 6. Moreover, the maximum interaction with  $\text{Ag}^+$  and **Z2** occurs at 0.5 mol fraction of **Z2**, thus confirming that it binds only a single silver cation (compare Figure S4 in the Supporting Information).

As such, the number of  $\text{Ag}^+$  cations captured by a given homologue of **Z1** (in Figures 6 and 7) is consistent with the fact that a pair of fluoranyl moieties is necessary for the effective capture of a single silver cation. As shown above in eqs 1 and 2, an efficient binding of  $\text{Ag}^+$  requires formation of a  $\pi$ -prismand-like cavity formed by three aromatic walls (i.e., two fluoranyl moieties and one xylil group). The oligomeric **Z<sub>n</sub>** exists in rapidly interconverting extended "Z" and folded "Δ" conformations in the absence of silver cations at 22 °C, as can be seen with the simple  $^1\text{H}$  NMR spectra (Figure S1 in the Supporting Information), and the conformational mobility of various oligomers (**Z<sub>n</sub>**) cannot be frozen at lower temperatures. However, introduction of  $\text{Ag}^+$  cations induces the folding of the various oligomers, containing an even number of fluorene moieties, by simple C–C bond rotations to produce 1, 2, 3, 4, and 5 deltaphane-like cavities in **Z1**, **Z3**, **Z5**, **Z7**, and **Z9**, respectively (i.e., see Figure 8 for a representative example).

The oligomers **Z2**, **Z4**, **Z6**, and **Z8**, containing an odd number of fluorene moieties form only 1, 2, 3, and 4 deltaphane-like cavities, respectively, upon exposure to a solution of  $\text{Ag}^+$  while leaving a single fluorene/xylene pair in an extended conformation (see Figure 8 for a representative example).

Note that the receptor site with an extended conformer binds silver cation with much less efficiency, i.e.,  $K \approx 10 \text{ M}^{-1}$  (see eq 3). It should be noted that the dynamic nature of silver-cation binding to various **Z<sub>n</sub>** would indicate that a single fluorene/xylene pair in an extended conformation is in continuous flux over the entire chain (vide infra).

The calculated AM1 structures (using Spartan) in Figure 8 together with the  $^1\text{H}$  NMR spectroscopic titrations data with  $\text{Ag}^+$  in Figure 6 and Job's plots in Figure 7 clearly account for the number of  $\text{Ag}^+$  cations captured by various oligomers **Z1**–**Z9**. Moreover, it is important to note that the simplicity of the  $^1\text{H}$  NMR spectra, obtained in the presence of varying equivalents of  $\text{Ag}^+$  (in Figures 4 and S7–S14 in the Supporting Information), suggests the dynamic nature of the binding of  $\text{Ag}^+$  to the multiple receptor sites of **Z2**–**Z9**.

Thus, a careful analysis of the changes in the chemical shifts of the xylene protons in the  $^1\text{H}$  NMR spectra of **Z3** obtained upon an incremental addition of  $\text{Ag}^+$  solution (vide infra) provides further insight into the dynamic nature of silver cation binding. As shown in Figure 9, the oligomer **Z3** can exist in at least four (almost) isoenergetic conformers (**Z3-A**, **Z3-B**, **Z3-C**, and **Z3-D**), as established by density function theory (DFT) calculations at the B3LYP/6-31G\* level.

On the basis of the number of observed (sharp) signals in the  $^1\text{H}$  NMR spectrum (see Figure S1 in the Supporting Information) of **Z3** it can be easily concluded that the almost isoenergetic conformers of **Z3** in Figure 9 are rapidly interconverting on the NMR time scale. The  $^1\text{H}$  NMR spectrum of **Z3**

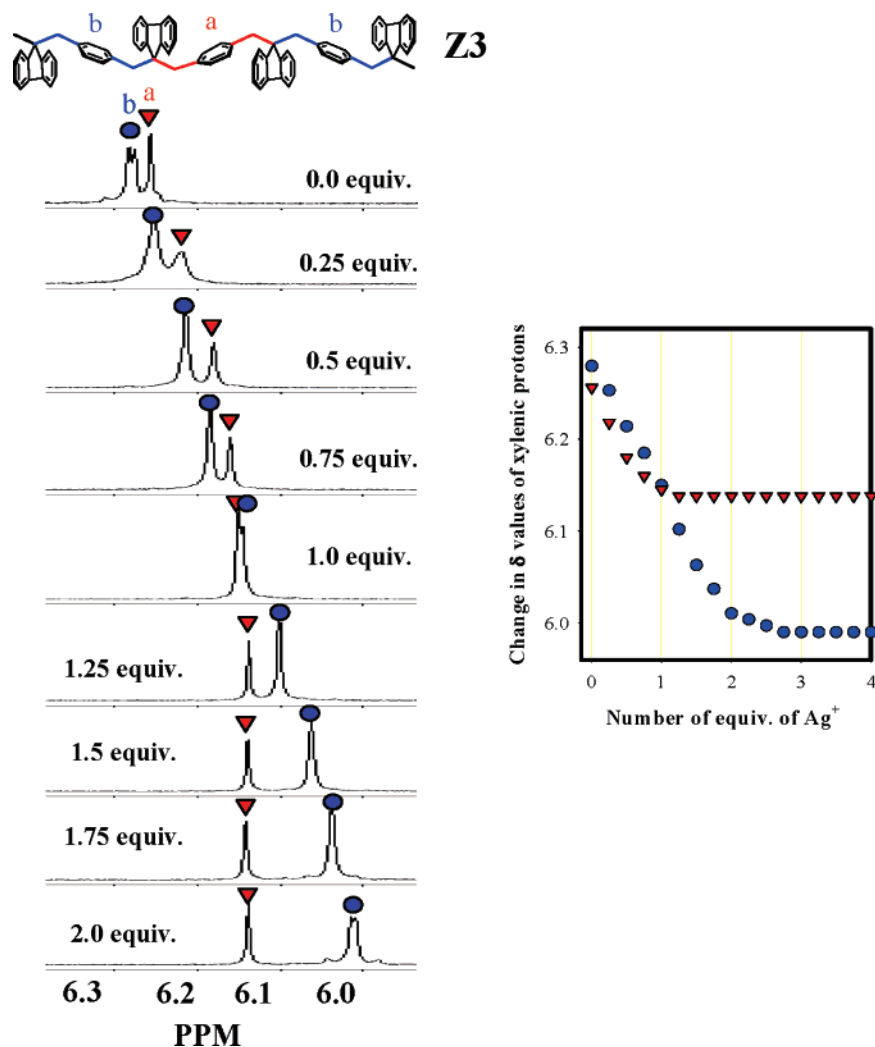
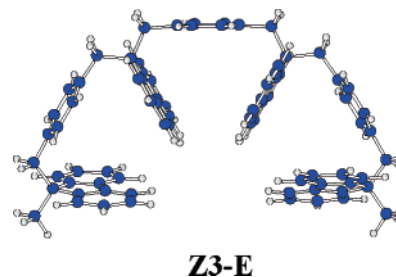


**Figure 10.** (Left) Partial  $^1\text{H}$  NMR spectra of **Z3** showing the changes in chemical shifts of xylenic protons upon incremental addition of  $\text{CF}_3\text{SO}_3^- \text{Ag}^+$  in  $\text{CDCl}_3\text{-CD}_3\text{OD}$  at  $22^\circ\text{C}$ . (Right) Plot of changes in the chemical shifts of xylenic protons (indicated by “a” and “b” in the structure in Figure 10) against the added equivalents of a solution of  $\text{CF}_3\text{SO}_3^- \text{Ag}^+$  in  $\text{CDCl}_3\text{-CD}_3\text{OD}$  at  $22^\circ\text{C}$ .

corresponds to a symmetrical structure in which a singlet from the inner xylenic protons (4H, indicated by ‘a’ in Figure 10) is readily distinguished from the distorted AB quartet from the outer xylenic protons (8H, indicated by ‘b’ in Figure 10). Figure 10 shows that both the xylenic signals from **Z3** shift upfield upon an incremental addition of up to 1 equiv of  $\text{Ag}^+$  cation. Moreover, the incremental addition of  $\text{Ag}^+$  beyond 1 equiv shows the upfield shift of only the outer xylenic protons up to addition of 2 equiv of silver cations, while the signal due to the inner xylenic protons remains unchanged (Figure 10).

The  $^1\text{H}$  NMR spectral change in Figure 10 can be easily reconciled with the aid of Scheme 3. Thus, exposure of **Z3** to 1 equiv of  $\text{Ag}^+$  will afford three possible structures containing a deltaphane-like cavity (i.e., **Z3-B**, **Z3-C**, and its mirror image **Z3-C'**) with equal probability, thus affecting the chemical shifts of all xylenic protons equally upon binding to the silver cation (see Figure 10, right). Note that the observation of only one set of signals in the  $^1\text{H}$  NMR spectrum indicates that all three silver-bound structures (i.e., **Z3-B**, **Z3-C**, and **Z3-C'**) are in dynamic equilibrium on the NMR time scale. Moreover, accommodation of a second silver cation in structures **Z3-B** or **Z3-C** or **Z3-C'** requires their transformation into a structure containing two deltaphane-like cavities in such a way that they are well

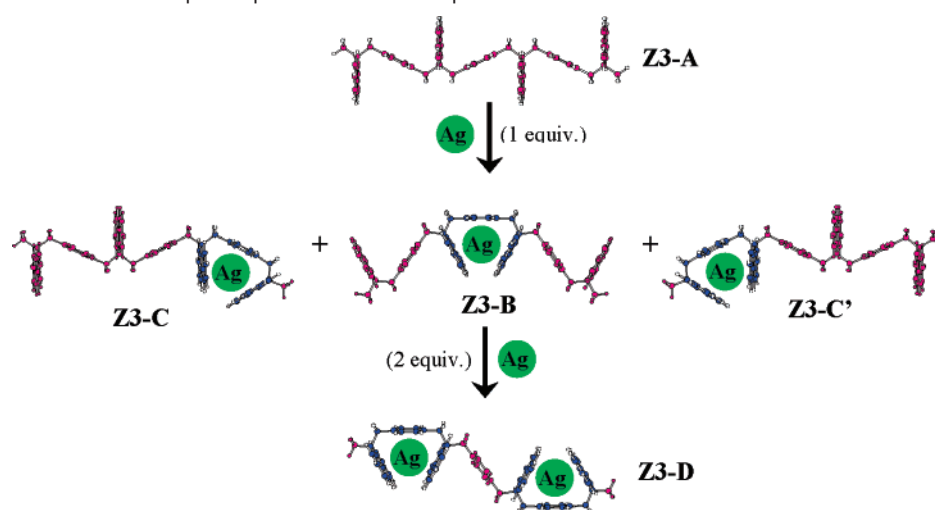
separated from each other to avoid Coulombic repulsion between the cationic guests, i.e., structure **Z3-D** in Scheme 3. Such an analysis is consistent with the fact that the chemical shift of only the outer xylenic protons should be affected upon binding of the second silver cation while the protons from the central xylene ring remain unaffected (see Figure 10). Note that an alternative structure **Z3-E** containing two deltaphane-like cavities is much higher in energy ( $\sim 5$  kcal/mol) compared to the structures in Figure 9 (or Scheme 3) as established by DFT calculations.



## Summary and Conclusions

We developed convergent syntheses of hitherto unknown fluorene-*p*-xylene oligomers **Z1–Z9** in excellent yields with



**Scheme 3.** Possible Structures of **Z3** upon Exposure to 1 and 2 Equiv of Silver Cations

the aid of four repetitive sequences of reactions, i.e., alkylation, lithium aluminum hydride reduction of benzoic esters, conversion of benzyl alcohols to benzyl chlorides using thionyl chloride, followed by alkylation as summarized in Scheme 2. These conformationally mobile and readily soluble oligomers, containing multiple receptor sites, were easily characterized by  $^1\text{H}$  and  $^{13}\text{C}$  NMR spectroscopy as well as mass spectrometry. The binding of multiple silver cations to **Z3–Z9** was possible due to the folding of these oligomers, by simple C–C bond rotations, to produce structures containing multiple deltaphane-like receptor sites (see Figure 8) for efficient binding of silver cations (i.e.,  $K \approx 15\,000\ \text{M}^{-1}$ ). The reproducible  $^1\text{H}$  NMR spectroscopic titration of the oligomers **Z1**, **Z3**, **Z5**, **Z7**, and **Z9** containing an even number of fluorene moieties confirmed that they bind 1, 2, 3, 4, and 5 silver cations, respectively, whereas oligomers **Z2**, **Z4**, **Z6**, and **Z8** containing an odd number of fluorene moieties bind 1, 2, 3, and 4 silver cations, respectively (see Figure 6). The number of  $\text{Ag}^+$  cations captured by various oligomers **Z1–Z9** is readily accounted for by the fact that introduction of  $\text{Ag}^+$  cations induces folding of the oligomers containing even number of fluorene moieties to produce 1, 2, 3, 4, and 5 deltaphane-like cavities in **Z1**, **Z3**, **Z5**, **Z7**, and **Z9**, respectively, whereas oligomers (**Z2**, **Z4**, **Z6**,

and **Z8**) containing odd number of fluorene moieties form 1, 2, 3, and 4 deltaphane-like cavities together with a single fluorene/xylene pair in an extended conformation. Note that the receptor site with an extended conformer binds silver cation with much less efficiency, i.e.,  $K \approx 10\ \text{M}^{-1}$  (see eq 3).

We are actively exploring the syntheses of the **Zn** analogues containing different substituents both on xylene and fluorene moieties to further modulate the binding and selectivity of various metal cations to these conformationally adaptable nanometer-sized materials with multiple metal binding sites.

**Acknowledgment.** We thank Dr. Ilia A. Guzei (University of Wisconsin at Madison) for the X-ray crystallography and the Petroleum Research Funds, administered by the American Chemical Society, and National Science Foundation (Career award) for financial support.

**Supporting Information Available:** Synthetic details,  $^1\text{H}/^{13}\text{C}$  NMR data for various intermediates,  $^1\text{H}$  NMR spectral titration data with silver cation, and X-ray structural data (PDF, CFIF). This material is available free of charge via the Internet at <http://pubs.acs.org>.

JA0687522